J Comp Physiol A (2002) 188: 611–620
DOI 10.1007/s00359-002-0336-4

ORIGINAL PAPER

M.A. Ashley-Ross · J.U. Barker

The effect of fiber-type heterogeneity on optimized work and power output of hindlimb muscles of the salamander *Ambystoma tigrinum*

Accepted: 16 July 2002 / Published online: 24 August 2002

Abstract Most vertebrate muscles are composed of a mixture of fiber types. However, studies of muscle mechanics have concentrated on homogeneous bundles of fibers. Hindlimb muscles of the tiger salamander, *Ambystoma tigrinum*, present an excellent system to explore the consequences of fiber heterogeneity. Isometric twitches and work loops were obtained in vitro from two muscles, the m. iliotibialis pars posterior (heterogeneous, containing types I, IIa and IIb fibers) and the m. iliofibularis (nearly homogeneous for type IIa fibers). Maximal isometric twitch and tetanic stresses in m. iliotibialis posterior were significantly greater than in iliofibularis. Work loops were obtained over a range of frequencies (0.5–3.0 Hz) and strains (2–6% muscle length) that encompassed the observed ranges in vivo. Work per cycle from the homogeneous iliofibularis declined from 1.5–3.0 Hz, while that from the heterogeneous m. iliotibialis posterior increased from 0.5 Hz to 2.5 Hz and declined at 3.0 Hz. Power output from the iliofibularis rose with frequency to at least 3 Hz; power from the iliotibialis posterior rose with frequency to 2.5 Hz and declined thereafter. Mass-specific work per cycle and power output were higher in iliofibularis than iliotibialis posterior over most frequencies and strains tested.

Keywords Fiber type · Muscle · Power output · Salamander · Work loop

Abbreviations *ILFB* m. iliofibularis · *ILTP* m. iliotibialis pars posterior · L_o muscle length

M.A. Ashley-Ross (✉) · J.U. Barker
Department of Biology, Box 7325,
Wake Forest University, Winston-Salem,
NC 27109, USA
E-mail: rossma@wfu.edu
Tel.: +1-336-7585529
Fax: +1-336-7586008

Introduction

Individual muscles may be made up of fibers which are all of one type (for example, white myotomal muscle in fish), or may be composed of a combination of fiber types, which may either be segregated from one another as in lizard m. iliofibularis (Jayne et al. 1990; Swoap et al. 1993), or intermingled with one another as in mammalian m. gastrocnemius (Weeks and English 1985). Muscle fibers of vertebrates are broadly categorized into type I (slow contracting, fatigue resistant) and type II (fast contracting). The type II fibers are further divided into type IIa, which are resistant to fatigue, and type IIb, which are fatigable but generate high forces (Burke 1981; Lieber 1992). Type I fibers are most prevalent in muscles involved in the maintenance of posture, while the type II fibers (particularly type IIb) are found in muscles that are used intermittently for tasks that require high forces (e.g., jumping; Smith et al. 1977).

Muscle function in a behavior is frequently studied using electromyography, which records the periods of activity for muscles involved during performance of the behavior. However, published electromyographic studies either do not discuss the fiber type compositions of the active muscles (for examples, see Engberg and Lundberg 1969; Wentink 1976; Rasmussen et al. 1978; Dial et al. 1991; Carrier 1993; Ashley-Ross 1995), or record preferentially from one type of fiber or another (lizard m. iliofibularis, Jayne et al. 1990; Johnson et al. 1994; fish myotomal muscle, Jayne and Lauder 1995). Equally important to a record of the motor pattern for an understanding of muscle function during behavior is a measure of work and power output by the muscle (Josephson 1985). Several researchers have attempted to link the contraction speed and power output characteristics of different vertebrate muscle fiber types to the performance of specific behaviors (e.g., Rome et al. 1988). However, measures of force-velocity relationships and work output by muscles during contraction

have been primarily restricted to bundles of homogeneous fibers (e.g., Harry et al. 1990; Warren et al. 1993; Wood et al. 1993; Barclay 1994). Likewise, reports of the consequences of muscle fiber type on functioning of the organism have thus far been restricted to fiber bundles that are homogeneous (Swoap et al. 1993; Johnson et al. 1994). However, many vertebrate locomotor muscles are composed of a mixture of fiber types, with each population having differing performance characteristics. Studies of a heterogeneous muscle were not able to reach firm conclusions on the consequences of fiber heterogeneity (Luiker and Stevens 1992, 1993), though it was suggested that the slower fibers in a heterogeneous muscle might degrade the performance of the fast fibers when the muscle is maximally activated. In no case have the consequences of fiber type heterogeneity been determined by comparing the contraction kinetics, work, and power output from muscles that are homogeneous in fiber type to muscles that are heterogeneous.

In this study, we examine the whole-muscle contractile characteristics and mechanical performance of two muscles from the hindlimb of the tiger salamander, *Ambystoma tigrinum*. The m. iliofibularis and extensor iliotibialis pars posterior are located in the thigh, on the postero-dorsal aspect of the femur (Fig. 1). They share similar parallel-fibered architectures and are of similar overall size, but they differ in their fiber composition. We show that the m. iliofibularis (ILFB) is composed almost entirely of type IIa fibers, while the m. iliotibialis pars posterior (ILTP) is composed of an almost equal mixture of type I, IIa, and IIb fibers. The two muscles also differ significantly in their performance, measured by both isometric tests and mechanical work and power output at several oscillation frequencies and strains. We relate these mechanical properties to the muscles' fiber composition and suggest correlations with muscle function during locomotion.

Fig. 1. Dorsal view of the superficial musculature of the right hindlimb of *Ambystoma tigrinum*. Anterior is toward the top of the figure. The m. iliotibialis pars posterior (*ILTP*), shown in blue, originates from the ilium and inserts on the tibial spine via a common tendon with the m. iliotibialis pars anterior. It is in a position to elevate the femur and extend the knee joint. The m. iliofibularis (*ILFB*), shown in red, originates on the ilium just posterior to the origin of the ILTP and crosses the posterior side of the knee joint to insert on the proximal fibula. It is in a position to elevate the femur, extend the hip joint, and flex the knee joint. Scale bar: 2 mm

Materials and methods

Animals

A. tigrinum, the tiger salamander, was chosen as the experimental animal as it has robust hindlimb muscles, many of which possess the same simple parallel-fibered architecture. All animals were obtained from Charles Sullivan Company (Nashville, Tenn., USA) as larvae, and then induced to metamorphose by addition of thyroxin to their aquarium water [three drops (approx. 0.15 ml) of 10 mg ml^{-1} stock solution added to 20 l of aquarium water daily]. Individuals were used for experiments within 1 month of metamorphosis. Salamanders were kept until use in 40-l aquaria half-filled with water and modified by addition of a moss-covered platform that allowed them access to land as they metamorphosed into the terrestrial form. To increase the rapidity with which they responded to the thyroxin, animals were not fed as larvae, but were fed a diet of crickets and earthworms after metamorphosis. The room in which the salamanders were housed was maintained on a 12 h:12 h light:dark photoperiod using broad-spectrum fluorescent lights that replicate the spectrum of sunlight.

Experimental protocol

Salamanders were anaesthetized by immersion in a solution of tricaine methane sulfonate (MS-222; 0.5 g l^{-1}) until the righting reflex was lost. The animal was then decapitated, and the pelvic region and hindlimbs were skinned. The muscle of interest (ILTP or ILFB; Fig. 1) was dissected out under Ringer's solution and removed along with a section of the ilium (origin for both muscles) and the tendon of insertion. The Ringer's solution contained (in mmol l^{-1}): NaCl, 145; KCl, 4; $CaCl_2$, 2.5; HEPES, 5. pH was adjusted to 7.0 at 20°C.

The muscle was placed in a Plexiglas chamber containing 40 ml of Ringer's solution with added glucose (2 g l^{-1}). Chamber temperature was maintained at 20°C by a water bath circulating fluid through a channel surrounding the experimental chamber. The

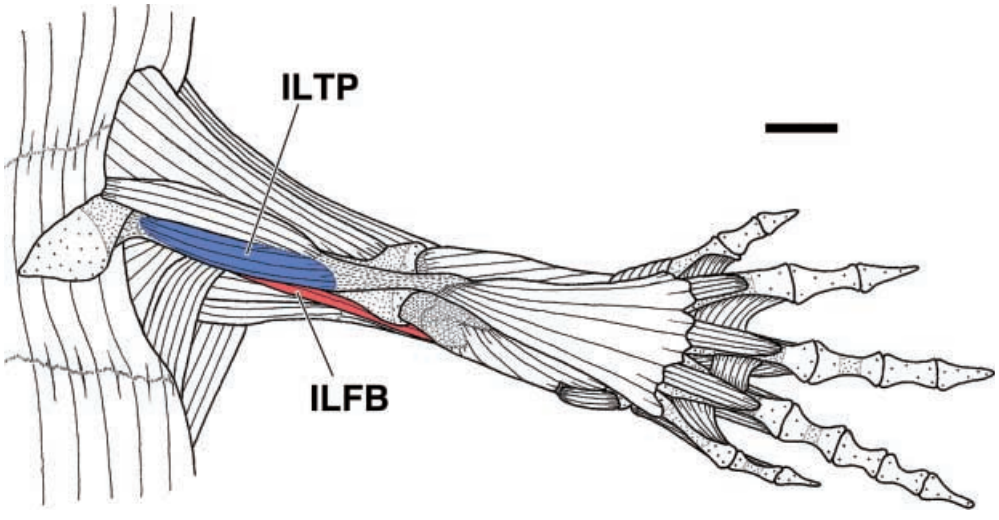

Ringer's solution was aerated throughout the experiment. The section of ilium was fixed in a stainless steel clamp in the lower part of the chamber, while silk suture was tied around the tendon of insertion and attached to the arm of a servomotor ergometer (Aurora Scientific, Ontario, Canada; model 300B) that also functioned as a force transducer. The ergometer was interfaced with a Macintosh PowerPC 8500 computer via a National Instruments data acquisition card (PCI-MIO-16XE-50). A custom-written LabVIEW (version 5.0, National Instruments, Austin, Tex., USA) program gathered force and position data and also commanded the servomotor position and triggered the stimulator. The muscle was stimulated to contract by a Grass S8800 stimulator (AstroMed-Grass, Quincy, Mass., USA) through silver plate electrodes placed in the bath on either side of the muscle. The sampling rate during all experiments was 1,000 samples/s.

Muscle length and stimulus strength were adjusted to produce maximal isometric twitch force. Muscle length (L_o) was then measured through a dissecting microscope using a digital micrometer. Mechanical work was measured using the work loop method (Josephson 1985). Briefly, the muscle was subjected to symmetrical sinusoidal length changes while being stimulated phasically at 100 Hz during the length change cycle. Plotting the record of muscle force versus length results in a loop-shaped trace. Because work is the product of force and distance, the area enclosed by the loop is the work performed by the muscle per cycle. Mechanical work and power output (work per cycle times oscillation frequency) were measured at six frequencies: 0.5 Hz, 1.0 Hz, 1.5 Hz, 2.0 Hz, 2.5 Hz, and 3.0 Hz. These length change frequencies were chosen as they completely encompass the range of limb cycling frequencies of salamanders during locomotion (Ashley-Ross 1994). Strain levels of 2%, 4% and 6% of L_o were selected because they completely overlap the range of calculated length change during a locomotor cycle. Lengths of the ILTP and ILFB were measured in animals that were fixed with the hindlimbs at angles corresponding to greatest and least length of the respective muscles during a step cycle. Both the ILFB and ILTP are bi-articular muscles, spanning both hip and knee joints, and because one of the joints is flexing while the other is extending, the muscles do not undergo much length change during a stride (measured strains of 5% in ILFB, 2% in ILTP). The phase of stimulation and duration of the pulse train were optimized to produce maximal work per cycle. The LabVIEW program generated a series of six consecutive length change cycles, and work per cycle was measured for cycles 3, 4, and 5 in the series, when work was relatively constant. Trials were separated by 5 min. Each muscle was tested at the three strains at two different frequencies. The experiment was ended when isometric tension fell below 80% of the initial value. Values for a particular frequency/strain combination represent the mean of data from four salamanders; a total of 20 salamanders were used for work-loop experiments.

Following each experiment, the muscle was frozen using liquid N_2 and tissue freezing medium and stored at –80°C. Subsequently, the muscle belly was sectioned at 20 μm on a Leica cryostat, and cross-sectional area was measured using image analysis software on a Zeiss light-phase microscope. Values for cross-sectional area are the mean of two sections for each muscle.

Data analysis

The following variables were analyzed for each muscle: maximum isometric twitch and tetanic stress, latency (time from rising edge of stimulus to the start of rise in force), time from stimulus to peak force, half-relaxation time, mean work per cycle, mean power output, and fiber type proportions. All variables except isometric twitch and tetanic stress and fiber type proportions were measured in LabVIEW. Maximum isometric stresses were calculated after measurement of muscle cross-sectional area. Fiber type composition was evaluated as described below. Data for the two muscles were analyzed for statistical significance in StatView for the Macintosh (version 5.0; SAS Institute, Cary, N.C., USA) using MANOVA for the isometric parameters, and three-way ANOVAs for work and power output that considered muscle, oscillation frequency, and strain as the main effects. Differences were considered significant at an $\alpha = 0.05$.

Muscle fiber typing

Fiber type composition was examined in sections of ILTP and ILFB from three animals. Muscles previously frozen in liquid N_2 and tissue freezing medium and stored at –80°C were sectioned at 20 μm on a Leica cryostat. Serial sections were processed for succinate dehydrogenase (SDH) to determine oxidative capacity and for myosin ATPase with acid pre-incubation at pH 4.6 (protocol developed by Vince Caiozzo at the University of California at Irvine). Pre-incubation at this pH differentiates between three fiber types in the muscle, corresponding to type I, IIa, and IIb (Vince Caiozzo, personal communication). Stained muscle sections were observed through a compound microscope and digital images of the sections were captured into a computer using a color video camera (Hitachi VK-C350). Fibers were counted in the public domain program NIH Image (developed at the US National Institutes of Health and available on the Internet at http://rsb.info.nih.gov/nih-image/).

Results

Fiber typing and isometric properties

The ILFB and ILTP have very different fiber type proportions, based on histochemical staining (Table 1, Fig. 2). The ILFB is composed nearly entirely of type IIa, or fast oxidative-glycolytic (FOG) fibers (mean 94% of the total), with an extremely small complement of type I, or slow oxidative (SO) fibers (mean 6%) (Fig. 2A, C). Additionally, the dark-staining type I fibers are much smaller in cross-sectional area than are the surrounding type IIa fibers. No ILFB sections examined contained any type IIb (fast glycolytic, FG) fibers. In contrast, the ILTP is composed of a more equal mix of type I (36%), type IIa (35%) and type IIb (29%) fibers (Fig. 2A, B). The length at which the ILTP produces maximum isometric force (L_o) is shorter than that of the ILFB, but the cross-sectional area of the ILTP is larger than that of the ILFB (Table 2). MANOVA performed on the isometric properties of the two muscles revealed a significant multivariate difference between them (Wilk's $\lambda = 0.34$, $F = 5.83$, $P = 0.0076$). Latency (time from stimulus initiation to the start of the rise in force) was significantly

Table 1. Fiber type composition of the M. extensor iliotibialis pars posterior (ILTP), and m. iliofibularis (ILFB) of *Ambystoma tigrinum*. Values are mean percentage (SD); $n = 3$ (*FG* fast glycolytic; *FOG* fast oxidative-glycolytic; *SO* slow oxidative)

	ILTP	ILFB
Type I (SO) *	36% (5.66%)	6% (1.00%)
Type IIa (FOG)**	35% (19.80%)	94% (1.00%)
Type IIb (FG)	29% (14.14%)	0%

*Significant difference between muscles; $F = 178.571$, $P < 0.0001$
**Significant difference between muscles; $F = 62.789$, $P = 0.0005$

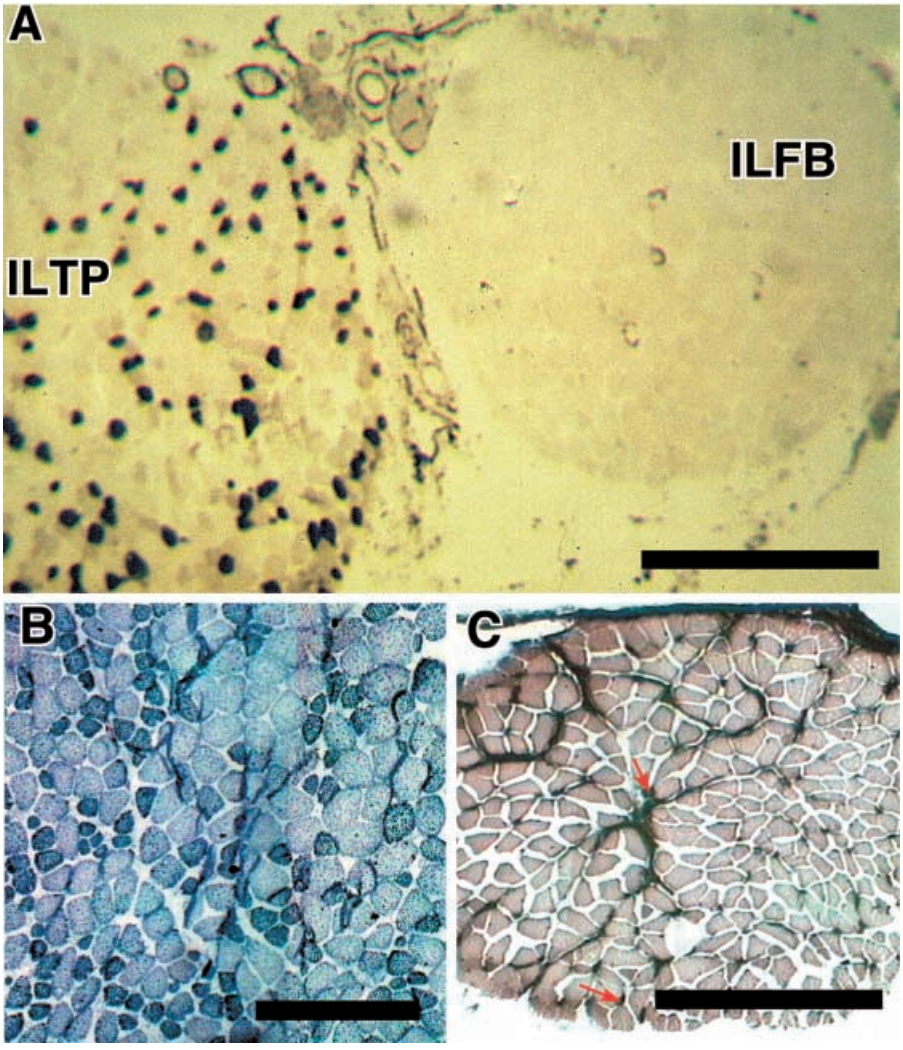

Fig. 2A–C. Microscopic sections of the ILTP and ILFB, stained to show different fiber types. **A** Both muscles on a single slide, stained for myosin ATPase activity with preincubation at pH 4.6. Type I fibers appear dark, type IIa fibers are lightly stained, and type IIb fibers are unstained. **B** Section through the ILTP, stained for succinate dehydrogenase (SDH) activity. Oxidative fibers appear dark. **C** Section through the ILFB, stained for myosin ATPase, pH 4.6 preincubation. Most of the cross-sectional area of the ILFB is composed of type IIa fibers. The few type I fibers present (dark; two are indicated by the *red arrows*) are extremely small in cross-section in comparison to the type IIa fibers. Scale bars are 0.5 mm in all panels

Table 2. Anatomical and isometric twitch parameters for the ILTP and ILFB. Values are given as mean (SD). For all ILTP values, $n = 12$; for all ILFB values, $n = 8$ (L_o muscle length)

	ILTP	ILFB	Results of single-factor ANOVAs	
			F	*P*
Cross-sectional area (mm^2)	0.4 (0.1)	0.2 (0.1)		
L_o (mm)	8.3 (1.0)	11.6 (1.6)		
Latency (ms)	8 (1)	9 (1)	9.689	0.0071
Time to maximum force (ms)	56 (9)	54 (5)	ns	ns
Half-relaxation time (ms)	41 (11)	63 (21)	3.670	0.0747
Maximum isometric twitch stress (kN m^{-2})	258 (46)	213 (12)	6.23	0.025
Maximum isometric tetanic stress (kN m^{-2})	361 (39)	302 (22)	7.42	0.011

different between the two muscles, with the ILTP beginning an increase in force earlier than the ILFB (Table 2). Maximum isometric stress (Fig. 3) also showed a significant difference, with the ILTP generating higher values than the ILFB (Table 2). The time to maximum force was nearly identical in the two muscles. Half-relaxation time was on average shorter in the ILTP than in the ILFB (see Fig. 3B), and this variable approached significance (Table 2).

Work and power output

Representative work loops from the ILTP and ILFB at several of the strain/frequency combinations tested are shown in Fig. 4. At 0.5 and 1.0 Hz, the ILFB did not maintain force throughout the shortening cycle, so no data for that muscle were analyzed at those frequencies. At all strains and frequencies tested, both muscles were capable of producing positive work with appropriate

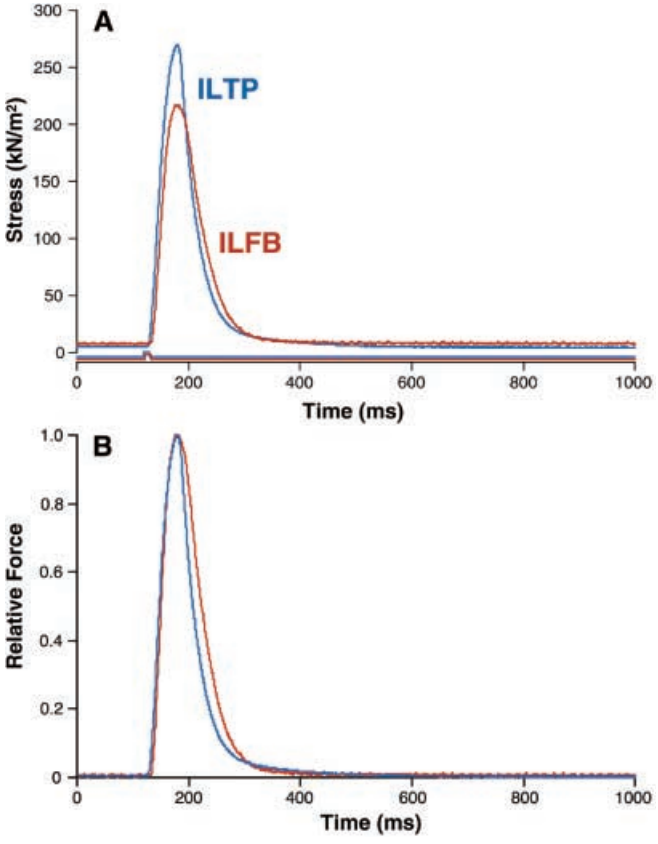

Fig. 3A,B. Representative isometric twitches from one ILTP (*blue*) and one ILFB (*red*). The small square pulse near the *x*-axis is the stimulus monitor. **A** Twitch stresses on an absolute scale. **B** The same traces scaled to percentage of maximum isometric twitch force

choice of stimulus duration and phase. The longer resting length of the ILFB is reflected in the greater *x*-axis excursion for its work loops. For both muscles, increasing strain from 2% to 4% of L_o resulted in nearly a doubling of the work per cycle; however, values at 6% strain do not correspond to a tripling of the work performed at 2% strain (Fig. 4). For both muscles, as cycling frequency increased (and thus cycle period decreased), the onset of stimulation for maximum work production shifted progressively into the lengthening part of the strain cycle. The duration of stimulation also decreased, and occupied less of the shortening phase, eventually ceasing while the muscle was still being lengthened (compare periods of stimulation between 1.5 Hz and 3.0 Hz; Fig. 4).

Average values of work per cycle (standardized to muscle volume) at the three strains and six frequencies tested are shown in Fig. 5. Work per cycle increased with strain, an effect that was most pronounced at lower frequencies. ANOVA demonstrated that work was significantly different between muscles, among strains, and among frequencies (Table 3). The significant muscle×frequency interaction term indicates that the two muscles behaved differently as oscillation frequency changed. The near-homogeneous ILFB exhibited a pattern of decreasing work per cycle with increasing frequency, with the highest values at 1.5 Hz for all three strains (means of 10.1 J kg^{-1}, 20.5 J kg^{-1}, and 23.9 J kg^{-1} at 2%, 4%, and 6% strain, respectively; Fig. 5). In contrast, the heterogeneous ILTP showed a pattern of increasing work per cycle as frequency increased from 0.5 Hz to 2.5 Hz, followed by a decline at 3.0 Hz (Fig. 5). The highest values of work per cycle in the ILTP occurred at 2.5 Hz for all three strains (means of 7.9 J kg^{-1}, 15.6 J kg^{-1}, and 19.8 J kg^{-1} at 2%, 4%, and 6% strain respectively; Fig. 5). The ILFB generated a greater amount of work per cycle than the ILTP at each frequency-strain combination (Fig. 5).

Figure 6 shows mean values for power output at the three strain levels and six cycling frequencies. ANOVA

Fig. 4. Representative work loops from the ILTP (*black*) and ILFB (*gray*) at three frequencies (*1.0 Hz*, *2.0 Hz*, and *3.0 Hz*) and three strain levels [*2%*, *4%*, and *6%* muscle length (L_o) total strain; i.e., 2% strain is ±1% of L_o]. ILFB typically had a longer L_o, reflected in the greater horizontal excursion of the gray traces. No data were collected at 1.0 Hz for the ILFB. The *thick regions* of the traces indicate when the muscle was being stimulated. Horizontal scale bar: 0.2 mm. Vertical scale bar: 100 mN

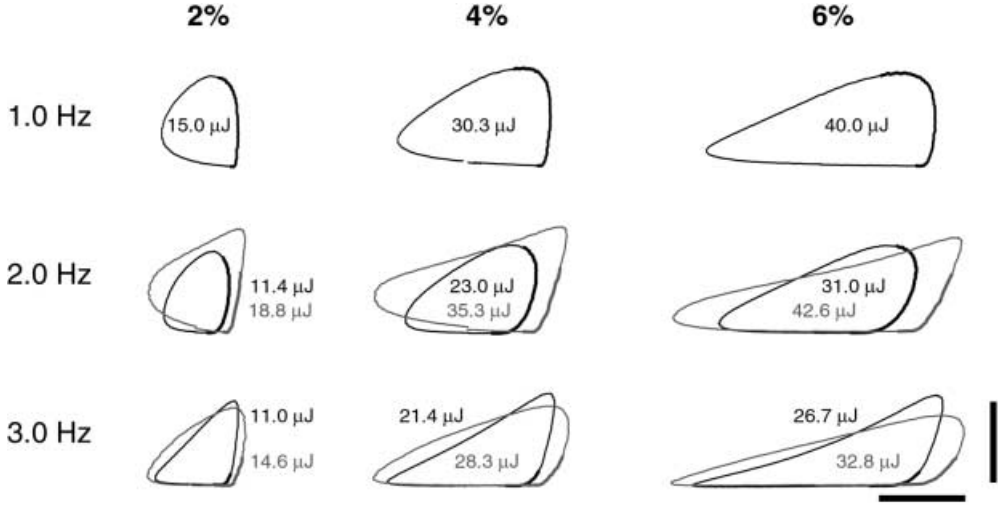

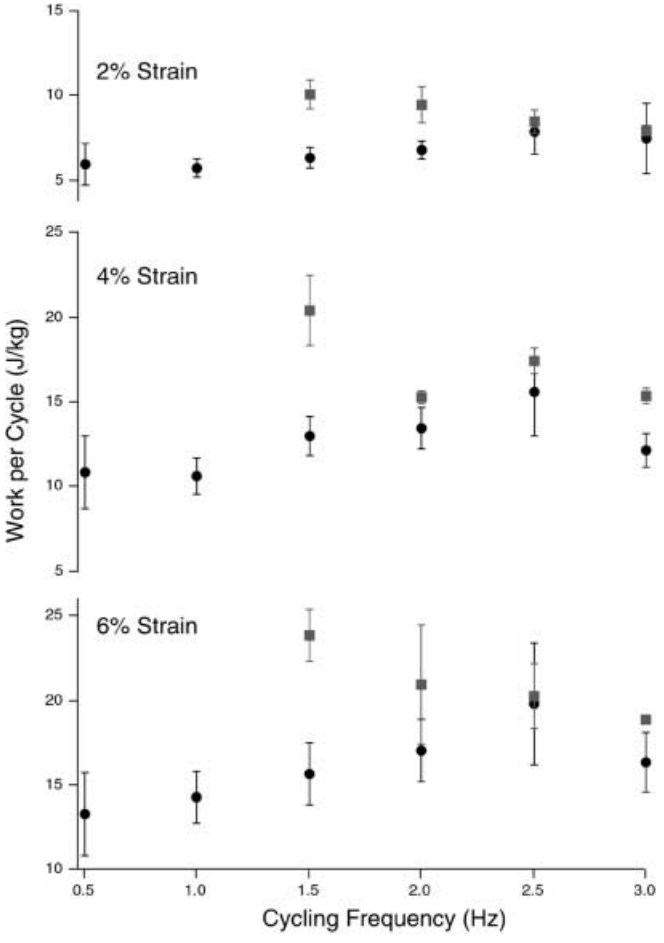

Fig. 5. Average work per cycle (J kg^{-1}) of the ILTP (*black circles*) and ILFB (*gray squares*) at six frequencies and three strains. Error bars represent one SEM. Some of the error bars are completely hidden by the symbols. No data were collected at 0.5 Hz and 1.0 Hz for the ILFB

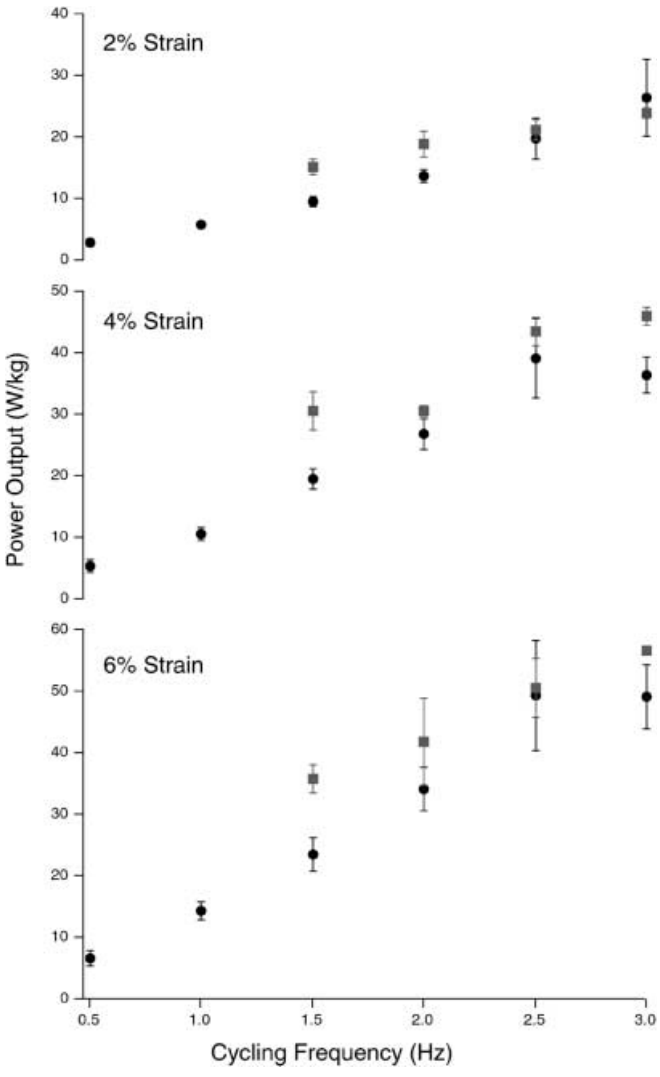

Fig. 6. Average power output (W kg^{-1}) of the ILTP (*black circles*) and ILFB (*gray squares*) at six frequencies and three strains. Error bars represent one standard error of the mean. Some of the error bars are completely hidden by the symbols. No data were collected at 0.5 Hz and 1.0 Hz for the ILFB

revealed that muscle, frequency, and strain were all significant effects (Table 4). Larger strains produced larger power outputs in both muscles (Fig. 6). Power output increased fairly steadily with frequency in the ILFB, but showed a peak at 2.5 Hz for the ILTP, with a decline in power output at 3.0 Hz for the 4% and 6% strain levels (Fig. 6). Both power output and work per cycle showed a significant decline between 2.5 Hz and 3.0 Hz, according to Fisher's protected least significant difference post-hoc test. At most of the frequency-strain combinations, the ILFB produced higher power output than the ILTP (Fig. 6).

Table 3. ANOVA results for work per cycle (in J kg^{-1}) of the ILTP and ILFB at three strains and four frequencies. Only significant results are shown

Effect	*F*	*P*
Muscle (*df* = 1)	16.308	0.0002
Frequency (*df* = 3)	10.441	< 0.0001
Strain (*df* = 2)	60.579	< 0.0001
Muscle×Frequency (*df* = 3)	4.325	0.0080

Discussion

Fiber type composition and isometric properties

The ILFB and ILTP differ significantly in their fiber compositions, with the ILFB being nearly homogeneous for type IIa fibers and the ILTP containing a mixture of

Table 4. ANOVA results for power output (in W kg^{-1}) of the ILTP and ILFB at three strains and four frequencies. Only significant results are shown

Effect	*F*	*P*
Muscle (*df* = 1)	10.353	0.0021
Frequency (*df* = 3)	20.802	< 0.0001
Strain (*df* = 2)	59.068	< 0.0001

type I, IIa, and IIb fibers (Table 1). The time-course of the isometric twitch in the two muscles also showed significant differences. The latency of the rise in force was extremely repeatable from trial to trial and between muscles (note small SD in Table 2), and was significantly shorter in the ILTP than the ILFB (Table 2), likely due to faster activation kinetics in the type IIb fibers of the ILTP. The time to maximum force was not significantly different in the two muscles. Half-relaxation time was shorter in the ILTP than in the ILFB (Table 2, Fig. 3B), again likely due to faster kinetics of the ILTP's type IIb fibers. The relaxation phase of the twitch of the ILFB can be fitted by a single exponential curve, reflecting the dominance of the single fiber type in this muscle (Fig. 7A). No improvement in fit is seen as a result of fitting the relaxation phase with a double or triple exponential curve. The initial falling phase of relaxation in the ILTP's twitch can also be fit with a single exponential curve (Fig. 7B), but the slow rate of fall at the end of the twitch fails to be adequately fit by a single or double exponential. However, fitting with a double or triple exponential curve does improve the fit (Fig. 7C, D), and in fact a triple exponential curve provides good agreement with the full relaxation phase of the ILTP twitch (Fig. 7D). We suggest that this reflects the contribution of the three distinct fiber types in this muscle to the twitch time-course. When MANOVA is used to test for overall differences in isometric twitch properties between the two muscles, a significant multivariate difference is revealed ($P = 0.0076$).

Patterns of work and power output in ILFB and ILTP in relation to fiber composition

The ILFB and ILTP differed significantly in the work per cycle and power they generated at three levels of muscle strain and four cycling frequencies (Tables 3, 4). Both muscles showed increased work and power output with increasing strain (Figs. 5, 6). The ILFB demonstrated a monotonic pattern of decreasing work with increasing frequency (Fig. 5), with the maximum mean work per cycle occurring at 1.5 Hz. However, power production showed the opposite pattern in the ILFB, increasing with oscillation frequency (Fig. 6). The ILFB is almost entirely homogeneous in fiber type, being composed of an average of 94% type IIa fibers (Table 1). The remaining 6% of the fibers are classified by histochemical staining as type I fibers; these fibers are much smaller in cross-sectional area than the type IIa fibers (Fig. 2C), and thus make a negligible contribution to the total cross-sectional area (and hence force) of the muscle. The pattern of a single maximum in work per cycle for the ILFB is likely a reflection of the domination of this muscle by a single fiber type.

ILTP shows a different pattern for work and power output, in each case with a maximum at 2.5 Hz (Figs. 5, 6). Is this peak indicative of the combined performance of the three fiber types in this muscle? Work loops performed in vitro measure the mechanical performance of the muscle in an artificial situation where all fibers are maximally activated (which may not reflect the in vivo stimulation pattern). Thus, as all fibers are contributing to force production, one would expect that even a heterogeneous muscle would show a single peak. Hill (1950) and others (e.g., Rome et al. 1988) have calculated that muscle fibers produce maximum power in the range of V/V_{max} (actual muscle shortening velocity over maximum shortening velocity) of 0.2–0.4. Red and white muscle fibers in fish are known to have very divergent V_{max} values (Rome et al. 1988), as are mammalian slow and fast muscle fibers (Rome et al. 1990). It is therefore likely that the three fiber types seen in this study also have different V_{max} values, and hence different speeds of shortening that correspond to the optimal V/V_{max} ranges. As cycling frequency increases, the more-powerful type IIa and IIb fibers may be working closer to their optimal shortening speeds, and consequently produce higher work and power values with increasing frequency. What then accounts for the decrease in work and power output at 3.0 Hz? The definitive cause remains to be determined, but two causes may be hypothesized. First, the slow type I fibers may be impeding the rest of the muscle due to their slow contractile kinetics, leading to reduced performance. Second, the non-contractile components may differ between ILFB and ILTP, such that these components in ILTP impede performance at frequencies above 2.5 Hz. These potential effects are not mutually exclusive and warrant further investigation.

The differing fiber compositions and work and power output patterns for the two muscles may be related to their function during locomotion. Kinematic and electromyographic data during treadmill locomotion are available for another species of salamander, *Dicamptodon tenebrosus,* that is similar to *Ambystoma* in overall size, body form, and muscle anatomy (Ashley-Ross 1992). In *Dicamptodon*, the ILFB is active primarily during the early part of the swing phase of the stride, and is one of two muscles active at that time that serve to lift the limb clear of the ground (Ashley-Ross 1995). The ILFB is thus required to be active during every stride, and lifts a constant amount of weight in a one-shot motion. A single fiber type that can contract quickly may be advantageous for this particular function. The ILTP plays a somewhat different role in the step cycle: it is active during the swing phase as the limb is being protracted (maintaining elevation of the femur), but it also shows a second burst of activity during the latter part of the stance phase in the majority of strides (Ashley-Ross 1995). During this time, the knee joint is extending to help propel the salamander forward, and the ILTP is the only muscle active in this period that could be responsible for this movement. As velocity of locomotion increases, the propulsive force required increases as well. The highest cycling frequencies tested (2.5 Hz and 3.0 Hz) lie above the range observed for steady walking, and correspond to those seen in escape

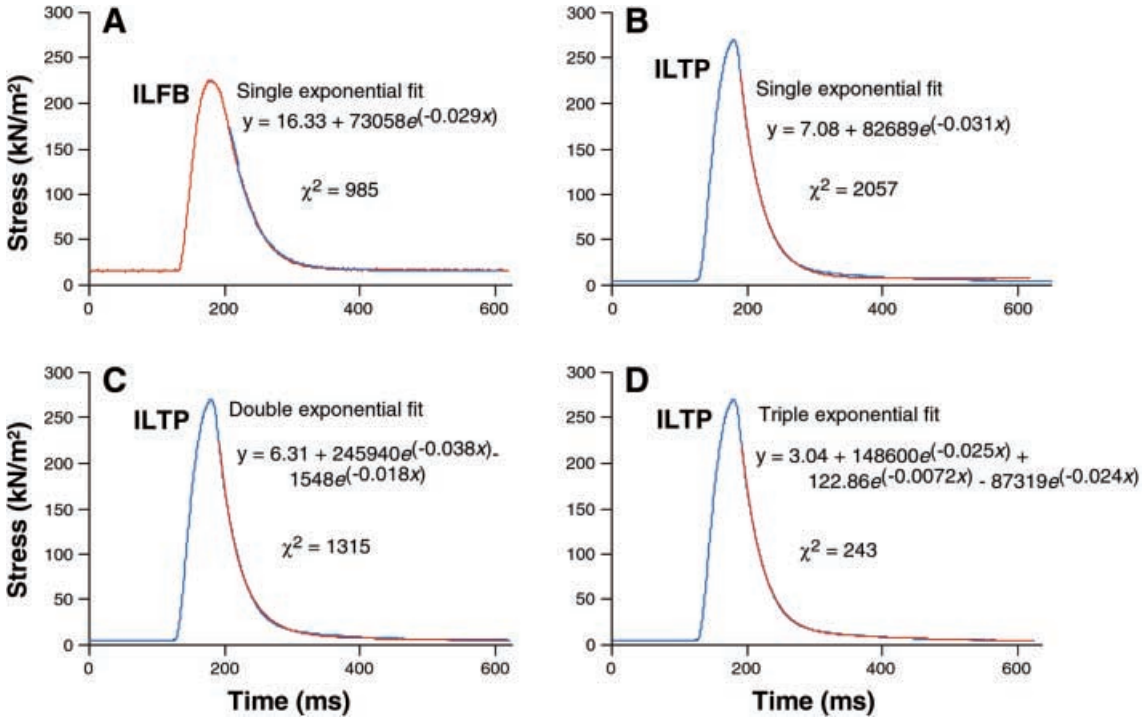

Fig. 7A–C. Exponential curve fits to the relaxation phase of isometric twitches. **A** A single exponential curve fits the relaxation of the ILFB. The χ^2 statistic encapsulates the summed deviation of the fitted curve from the raw data. Smaller χ^2 values indicate a better fit. Double and triple exponential curves fitted to the ILFB resulted in no decline in the χ^2 value. **B** A single exponential curve fitted to the relaxation phase of the ILTP fails to adequately describe the latter part of the relaxation of the ILTP twitch. Note the higher χ^2 value than for the ILFB. **C** A double exponential curve improves the fit to the relaxation phase of the ILTP twitch (note decrease in χ^2). **D** A triple exponential curve provides further improvement in the curve fit (smallest χ^2 value observed). ILFB twitch is shown in *red*, ILTP twitches are shown in *blue*, and the fitted curves are plotted in the opposite color in each panel

locomotion. The peak power output at 2.5 Hz may thus be indicative of the contribution of the type IIb fibers to very fast movements used during an escape response.

Comparisons to other muscles

Most studies of mechanical work and power output using the work loop method have been performed on bundles of muscle fibers that are homogeneous in fiber type. An exception is the series of studies by Luiker and Stevens (1992, 1993) on the mechanical properties of the pectoral fin adductor muscle of the pumpkinseed sunfish, *Lepomis gibbosus*. This muscle contains approximately 55% anaerobic fibers and 45% fibers that stain for SDH at varying intensities, and thus a range of aerobic capacities (Luiker and Stevens 1992). While differing from the fiber composition of the ILTP (nearly equal proportions of type I, IIa and IIb fibers), it is nonetheless instructive to compare mechanical performance of the *Lepomis* pectoral adductor muscle with that of the salamander ILTP. Maximal isometric stress was lower in the pectoral fin adductor (177 kN m^{-2}; Luiker and Stevens 1992) than in ILTP. Tetanic stress values of the pectoral fin adductor muscle (Luiker and Stevens 1992) were intermediate between those of fish red and white myotomal muscle (Altringham and Johnston 1988; Rome and Sosnicki 1990), reflecting its heterogeneous composition. The range of cycle frequencies tested by Luiker and Stevens (1992, 1993) overlapped at the low end with those used in this study (1 Hz and 2 Hz), and the strain used (6% L_o) matched the longest strain used here. The *Lepomis* pectoral fin adductor muscle generated work per cycle and power with values lower than those of the tiger salamander muscles at 1.0 Hz and 2.0 Hz (range of 2.5–6.2 J kg^{-1} at 1.0 Hz, 3.2–5.5 J kg^{-1} at 2.0 Hz (Luiker and Stevens 1993). Over the range of 1–8 Hz, the pectoral adductor showed a single peak in power output and a steady decrease in work per cycle with increasing frequency (Luiker and Stevens 1993). Values for the ILTP in this study show the same pattern for power output, but a different one for work per cycle, than seen in the pumpkinseed sunfish.

The cycling frequency that produced maximum power output in the *Ambystoma* ILTP (2.5 Hz) was lower than optimal cycling frequencies reported for other vertebrate locomotor muscles tested. For example, red myotomal muscle from fish typically produces maximum power output at 3–5 Hz (Johnson et al. 1994; Rome and Swank 1992), slow deep myotomal muscle from tuna and bonito at 4–6 Hz (Altringham and Block 1997), lizard iliofibularis at 3–20 Hz (Swoap et al. 1993), mouse soleus at 5 Hz (James et al. 1995), and mouse extensor digitorum longus at 10 Hz (James

Table 5. Comparative values of isometric parameters, work and power output from representative vertebrate skeletal muscles

Muscle	Temperature (°C)	Max work per cycle (J kg^{-1})	Max power output (W kg^{-1})	Reference
Ambystoma ILFB	20	23.9 (1.5 Hz)	56.7 (3.0 Hz)	This study
Ambystoma ILTP	20	19.8 (2.5 Hz)	49.5 (2.5 Hz)	This study
Lepomis pectoral fin adductor	14	6.2 (1 Hz)	26.7 (5 Hz)	Luiker and Stevens (1993)
Stenotomus chrysops red myotome	20	10.9 (5 Hz)	27.9 (5 Hz)	Rome and Swank (1992)
Micropterus salmoides red myotome	20	4.3 (1 Hz)	10.6 (3 Hz)	Johnson et al. (1994)
Thunnus albacares slow fibers	20		6.5 (4 Hz)	Altringham and Block (1997)
Sarda chiliensis slow fibers	20		11 (5 Hz)	Altringham and Block (1997)
Dipsosaurus dorsalis iliofibularis	22	7.6 (5.9 Hz)	42.6 (5.9 Hz)	Swoap et al. (1993)

et al. 1995). In the studies listed, temperature affects optimal cycling frequency such that the two are positively correlated. Because no frequency greater than 3.0 Hz was tested in the present study, it cannot be determined whether the power output from ILFB at that frequency is truly maximal for the muscle. Values for maximal work and power output for both the ILFB and ILTP are similar to those obtained from other muscles at similar temperature and cycling frequency (Table 5).

Salamanders do not walk or trot at particularly high speeds; a typical walking velocity is approximately 0.7 SVL s^{-1}, and limb cycling frequency is approximately 1 Hz (Ashley-Ross 1994). Thus, it is perhaps not surprising that the optimal cycling frequencies for the muscles tested were lower than muscles from other groups that conduct faster locomotion. However, within the restricted range of frequencies tested, the heterogeneous ILTP appears to follow the basic recruitment order seen in studies of speed-induced motor pattern changes in mammals. In cat superficial ankle extensors, at slow walking speeds the majority of the force is produced by type I fibers, with only a small contribution from type IIa fibers (Smith et al. 1977). As speed increases, the faster fiber types make an increasing contribution to total force production (Armstrong et al. 1977). This same general pattern may be present in the ILTP, with the largest contribution to force at low cycling frequencies (equivalent to low walking speeds) coming from the type I fibers; the type IIb fibers would be expected to fatigue quickly, and thus contribute little to the overall force for the cycle. At the other extreme, at high cycling frequencies (equivalent to an escape response), the time over which the limb is in contact with the ground is short, and thus muscular force must be high to adequately propel the animal. At these frequencies, the type IIb fibers are providing the majority of the force, and the slower fibers are essentially pulled along by the faster fibers. Indeed, at higher frequencies the type I fibers may be still contracting while the muscle is being re-lengthened, and therefore may contribute to negative work done by the muscle (see Fig. 4, 1.5 Hz and 2.0 Hz; elevated force as the muscle is being lengthened toward L_o from its shortest length).

The ILFB and ILTP are parallel-fibered muscles in the salamander hindlimb that differ in their fiber composition, isometric properties, and in vitro work and power output. The homogeneous (type IIa) ILFB shows a simple pattern of decreasing work per cycle with increasing frequency and increasing power output. However, the heterogeneous extensor ILTP shows a complex relationship between work, power, and cycling frequency, which we suggest is the result of the mixture of fiber types present in this muscle. This suggests that heterogeneous muscle function during locomotion will be similarly complex.

Acknowledgements This work was supported by grant IBN-9813730 from the National Science Foundation to M.A. A-R, and a Sullivan Scholarship from Wake Forest University to J.U.B. The experiments performed in this study were approved by the Animal Care and Use Committee of Wake Forest University, comply with both the "Principles of Animal Care," publication No. 86-23, revised 1985, of the National Institutes of Health and also with the current laws of the United States of America.

References

Altringham JD, Block BA (1997) Why do tuna maintain elevated slow muscle temperatures? Power output of muscle isolated from endothermic and ectothermic fish. J Exp Biol 200:2617–2627

Altringham JD, Johnston IA (1988) The mechanical properties of polyneuronally innervated, myotomal muscle fibres isolated from a teleost fish (*Myoxocephalus scorpius*). Pflugers Arch 412:524–529

Armstrong RB, Marum P, Saubert CW, Seeherman HJ, Taylor CR (1977) Muscle fibre activity as a function of speed and gait. J Appl Physiol 43:672–677

Ashley-Ross MA (1992) The comparative myology of the thigh and crus in the salamanders *Ambystoma tigrinum* and *Dicamptodon tenebrosus*. J Morphol 211:147–163

Ashley-Ross MA (1994) Hindlimb kinematics during terrestrial locomotion in a salamander *(Dicamptodon tenebrosus)*. J Exp Biol 193:255–283

Ashley-Ross MA (1995) Patterns of hind limb motor output during walking in the salamander *Dicamptodon tenebrosus,* with comparisons to other tetrapods. J Comp Physiol A 177:273–285

Barclay CJ (1994) Efficiency of fast- and slow-twitch muscles of the mouse performing cyclic contractions. J Exp Biol 193:65–78

Burke RE (1981) Motor units: anatomy, physiology, and functional organization. In: Brooks VB (ed) Handbook of physiology. American Physiological Society, Bethesda, MD, pp 345–422

Carrier DR (1993) Action of the hypaxial muscles during walking and swimming in the salamander *Dicamptodon ensatus*. J Exp Biol 180:75–83

Dial KP, Goslow GE, Jenkins FA (1991) The functional anatomy of the shoulder in the European starling *(Sturnus vulgaris)*. J Morphol 207:327–344

Engberg I, Lundberg A (1969) An electromyographic analysis of muscular activity in the hindlimb of the cat during unrestrained locomotion. Acta Physiol Scand 75:614–630

Harry JD, Ward AW, Heglund NC, Morgan DL, McMahon TA (1990) Cross-bridge cycling theories cannot explain high-speed lengthening behavior in frog muscle. Biophys J 57:201–208

Hill AV (1950) The dimensions of animals and their muscular dynamics. Sci Prog 38:209–230

James RS, Altringham JD, Goldspink DF (1995) The mechanical properties of fast and slow skeletal muscles of the mouse in relation to their locomotory function. J Exp Biol 198:491–502

Jayne B, Lauder G (1995) Red muscle motor patterns during steady swimming in largemouth bass: effects of speed and correlations with axial kinematics. J Exp Biol 198:1575–1587

Jayne BC, Lauder GV, Reilly SM, Wainwright PC (1990) The effect of sampling rate on the analysis of digital electromyograms from vertebrate muscle. J Exp Biol 154:557–565

Johnson TP, Syme DA, Jayne BC, Lauder GV, Bennett AF (1994) Modeling red muscle power output during steady and unsteady swimming in largemouth bass. Am J Physiol 267:R481–488

Josephson RK (1985) Mechanical power output from striated muscle during cyclic contraction. J Exp Biol 114:493–512

Lieber RL (1992) Skeletal muscle structure and function: implications for rehabilitation and sports medicine. Williams and Wilkins, Baltimore

Luiker EA, Stevens ED (1992) Effect of stimulus frequency and duty cycle on force and work in fish muscle. Can J Zool 70:1135–1139

Luiker EA, Stevens ED (1993) Effect of stimulus train duration and cycle frequency on the capacity to do work in the pectoral fin muscle of the pumpkinseed sunfish, *Lepomis gibbosus*. Can J Zool 71:2185–2189

Rasmussen S, Chan AK, Goslow GE (1978) The cat step cycle: electromyographic patterns for hindlimb muscles during posture and unrestrained locomotion. J Morphol 155:253–269

Rome LC, Sosnicki AA (1990) The influence of temperature on mechanics of red muscle in carp. J Physiol (Lond) 427:151–170

Rome LC, Swank D (1992) The influence of temperature on power output of scup red muscle during cyclical length changes. J Exp Biol 171:261–281

Rome LC, Funke RP, Alexander RM, Lutz G, Aldridge H, Scott F, Freadman M (1988) Why animals have different muscle fibre types. Nature 335:824–827

Rome LC, Sosnicki AA, Goble DO (1990) Maximum velocity of shortening of three fiber types from horse soleus. J Physiol (Lond) 431:173–186

Smith JL, Edgerton VR, Betts B, Collatos TC (1977) EMG of slow and fast ankle extensors during posture, locomotion and jumping. J Neurophysiol 40:503–513

Swoap SJ, Johnson TP, Josephson RK, Bennett AF (1993) Temperature, muscle power output and limitations on burst locomotor performance of the lizard *Dipsosaurus dorsalis*. J Exp Biol 174:185–197

Warren GL, Hayes DA, Lowe DA, Armstrong RB (1993) Mechanical factors in the initiation of eccentric contraction-induced injury in rat soleus muscle. J Physiol (Lond) 464:457–475

Weeks OI, English AW (1985) Compartmentalization of the cat lateral gastrocnemius motor nucleus. J Comp Neurol 235:255–267

Wentink GH (1976) The action of the hind limb musculature of the dog in walking. Acta Anat 96:70–80

Wood SA, Morgan DL, Proske U (1993) Effects of repeated eccentric contractions on structure and mechanical properties of toad sartorius muscle. Am J Physiol 265:C792–C800